BNL-66325

RETRIEVAL OF OPTICAL PROPERTIES OF ATMOSPHERIC AEROSOLS FROM MOMENTS OF THE PARTICLE SIZE DISTRIBUTION

Douglas L. Wright, Jr.
Environmental Chemistry Division
Department of Applied Science
Brookhaven National Laboratory
Upton, NY 11973-5000

Original Manuscript Date: February 1999

Published in
Journal of Aerosol Science
31, 1-18, 2000

This research was performed under the auspices of the U.S. Department of Energy under Contract No. DE-AC02-98CH10886.

Pergamon

www.elsevier.com/locate/jaerosci

PII: S0021-8502(99)00028-2

J. Aerosol Sci. Vol. 31, No. 1, pp. 1–18, 2000
Published by Elsevier Science Ltd
Printed in Great Britain
0021-8502/99/$ - see front matter

RETRIEVAL OF OPTICAL PROPERTIES OF ATMOSPHERIC AEROSOLS FROM MOMENTS OF THE PARTICLE SIZE DISTRIBUTION

Douglas L. Wright, Jr.

Environmental Chemistry Division, Department of Applied Science, Brookhaven National Laboratory, Upton, NY 11973, U.S.A.

(*First received* 26 *October* 1998; *and in final form* 16 *February* 1999)

Abstract—A technique is described for efficient retrieval of families of smooth model distributions, such as lognormals or modified gammas, from the lower moments of the particle size distribution from which aerosol optical properties can be accurately computed. The Multiple Isomomental Distribution Aerosol Surrogate (MIDAS) technique, along with the quadrature technique of McGraw *et al.* (1995 *Geophys. Res. Lett.* **22,** 2929–2932), is evaluated by computing the extinction efficiency, asymmetry parameter, backscatter fraction, 180° backscattering cross section, upscatter fraction, mass scattering efficiency, and a direct shortwave forcing at 8 wavelengths for 28 test distributions derived from field observations of marine, continental, urban and stratospheric aerosols. For the 224 single wavelength evaluations with retrieved modified gammas the average magnitude of error for each of the computed optical properties was 2% or less, with the exception of the 180° backscattering cross section (4%), establishing the accuracy of the technique. It is concluded that this approach is useful for obtaining aerosol optical properties from the first 6 moments of the size distribution, permitting confident determination of these properties from models in which aerosol evolution is represented by evolution of the lower-order moments. Published by Elsevier Science Ltd

1. INTRODUCTION

There is currently a growing need to represent aerosols and their evolution processes in atmospheric chemistry and transport models, especially regarding their radiative effects on climate. Most current models explicitly represent the aerosol size distribution with either discrete size bins (the sectional representation) or with assumed functional forms for various modes in the distribution (the modal approach). These are standard modeling schemes well-investigated in the literature. More recently, there has been exploration of representing aerosols by the moments of the size distribution alone, without the necessity of representing the size distribution itself. Moment-based approaches initially suffered from the necessity of assuming certain functional forms for the size distribution in order to obtain a closed set of moment evolution equations. However, with the introduction of the quadrature techniques of McGraw (1997) and Barrett and Webb (1998), condensational growth laws or coagulation kernels of arbitrary functional form became simple to treat with low-order moments and the method of moments became a viable candidate for modeling aerosols under very general conditions. The advantages of modeling aerosols with their lower-order moments rather than the full size distribution itself has been discussed by McGraw *et al.* (1995, 1998), McGraw (1997), Barrett and Webb (1998) and elsewhere. Aerosol dynamics via the Quadrature Method of Moments of McGraw (1997) has now been incorporated in the Eulerian chemical transport and transformation model of Benkovitz *et al.* (1994) and we will report on such simulations in the near future.

Given these efforts in modeling atmospheric aerosols for climate studies, successful modeling with moments requires aerosol optical properties and radiative influence to be accurately and efficiently computed from modeled moments. More specifically, one wants to know to what extent, if any, knowledge of only the lower-order moments rather than the size distribution itself results in significant additional uncertainties in computed aerosol optical properties. One of the findings of this study is that the additional uncertainties are

small, especially in light of uncertainties in large-scale modeling and the uncertainties in present knowledge of atmospheric aerosols.

Although optical properties can to some extent be related directly to the lower-order moments themselves, a more general approach utilizing moments is desirable. McGraw *et al.* (1995) initiated work along this line introducing a Gaussian quadrature technique, and Yue *et al.* (1997) extended the Randomized Search Minimization Technique of Heintzenberg *et al.* (1981) to the retrieval of optical properties from moments. The N abscissas and weights of the N-point quadrature technique may be viewed as an N-disperse representation of the underlying distribution and the Randomized Search Minimization Technique retrieves a histogram representation of the distribution as an intermediate step to the computation of optical properties.

This work introduces the Multiple Isomomental Distribution Aerosol Surrogate (MIDAS) technique. "Surrogate" indicates that the technique does not purport to retrieve the "true" distribution, but rather an isomomental surrogate suitable for use in integrals over the size distribution. Recognizing that it is integrals over the size distribution that are needed makes it understandable that isomomental surrogates are successful. In this work the surrogates are multimodal lognormal or multimodal modified gamma distributions. As smooth particle size distributions are the natural result of the generation and transformation processes that govern atmospheric aerosols, we anticipate that the use of these smooth model distributions will be advantageous. The quadrature approach of McGraw *et al.* (1995) is obtained as a limiting case of the lognormal version of the MIDAS technique and is evaluated alongside the present approach for the determination of aerosol optical properties.

Although we are concerned primarily here with modeled aerosols, another potential future application is the computation of aerosol optical properties from moments retrieved from remote sensing observations, such as multiwavelength extinction measurements (Livingston and Russell, 1989; Kaufman *et al.*, 1997). Recent satellite observations (Deuze *et al.*, 1998; Goloub *et al.*, 1998) provide measurements of the angstrom exponent [d log(optical depth)/d log(wavelength)] and other optical properties that will be useful in evaluating 3-D aerosol models that permit accurate retrieval of these properties.

2. METHOD

For a size distribution $f(r)$ of spherical particles of radius r the radial moments are defined as

$$\mu_k = \int_0^\infty r^k f(r)\,\mathrm{d}r, \tag{1}$$

and in this work they are computed from test distributions derived from field measurements. Aerosol optical properties are obtained by first retrieving a set, or family of smooth model distributions, each member of which having the specified moments. These retrieved model distributions are then averaged and optical properties are computed from the average-retrieved distribution. Standard methods can be used to obtain optical properties from the averaged-retrieved distributions. Simple discretization on a logarithmic scale has been used in this work to evaluate integrals over the size distribution, although more efficient standard quadrature techniques might be employed.

2.1. *Retrieval technique*

The normalized lognormal distribution

$$f_{\mathrm{LN}}(r) = \frac{1}{\mathrm{r}\ln\sigma\sqrt{2\pi}}\exp\left[-\frac{1}{2}\left(\frac{\ln(r/R)}{\ln\sigma}\right)^2\right] \tag{2}$$

with geometric mean radius R and geometric standard deviation on σ has radial moments

$$\mu_k^{\mathrm{LN}} = R^k \exp\left[\frac{k^2}{2}(\ln \sigma)^2\right] = R^k\, S^{\mathrm{LN}}(k; \sigma)\,, \tag{3}$$

and the normalized modified gamma distribution

$$f_{\mathrm{MG}}(r) = \frac{s\, b^{(n+1)/s}\, r^n}{\Gamma[(n+1)/s)]} \exp(-b\, r^s) \tag{4}$$

has radial moments

$$\mu_k^{\mathrm{MG}} = \frac{b^{-k/s}\, \Gamma[(k+n+1)/s]}{\Gamma[(n+1)/s]} = (b^{-1/s})^k\, S^{\mathrm{MG}}(k; n, s)\,. \tag{5}$$

A bimodal lognormal is a 6-parameter distribution and in principle can be fit to 6 moments of a size distribution. Although it would be highly desirable to *algebraically* solve for the lognormal (or other model distribution) parameters in terms of the 6 moments, to our knowledge this has not been achieved. Unsuccessful attempts to accomplish this led to the following mathematical device.

For a *trimodal* lognormal

$$f(r) = N_1 f_{\mathrm{LN}}^{(1)}(r) + N_2 f_{\mathrm{LN}}^{(2)}(r) + N_3 f_{\mathrm{LN}}^{(3)}(r) \tag{6}$$

the moments are

$$\mu_k = N_1\, R_1^k\, S^{\mathrm{LN}}(k; \sigma_1) + N_2\, R_2^k\, S^{\mathrm{LN}}(k; \sigma_2) + N_3\, R_3^k\, S^{\mathrm{LN}}(k; \sigma_3) \tag{7}$$

where N_1, N_2 and N_3 are the numbers of particles, R_1, R_2 and R_3 the geometric mean radii, and σ_1, σ_2 and σ_3 the geometric standard deviations of modes 1, 2 and 3, respectively. There are 9 lognormal parameters, allowing 3 constraints to be imposed while seeking a fit to the first 6 moments, $k = 0 - 5$. Let $\sigma_1 = \sigma_2 = \sigma_3 \equiv \sigma$ be a "retrieval parameter" and define the *pseudo-moments* as

$$\omega_k = \frac{\mu_k}{S^{\mathrm{LN}}(k; \sigma)}\,. \tag{8}$$

We then get

$$\omega_k = N_1\, R_1^k + N_2\, R_2^k + N_3\, R_3^k\,, \tag{9}$$

and with a change of symbols

$$\omega_k = w_1\, r_1^k + w_2\, r_2^k + w_3\, r_3^k\,. \tag{10}$$

For the purposes of *rapidly* solving equation (10) for the unknown lognormal parameters, this set of equations is now interpreted as defining the 3-point Gaussian quadrature weights and abscissas (with unknown weight function) appropriate to the given set of moments, and a routine such as ORTHOG of Press *et al.* (1992) will quickly deliver the $\{w_i, r_i\}$. The lognormal parameters are then obtained as

$$N_i = w_i\,, \quad R_i = r_i\,, \quad \sigma_i = \sigma \text{ retrieval parameter.} \tag{11}$$

The retrieval parameter σ cannot be chosen arbitrarily large or ORTHOG may not yield the desired weights and abscissas. This is apparently due to the fact that for σ too large the pseudo-moments fail to satisfy a convexity criterion that must be met by any valid set of moments of a distribution of a random variable (Feller, 1971). For example, if a lognormal test distribution is used to compute a set of moments, the retrieval parameter σ employed apparently cannot be larger than the geometric standard deviation of the test distribution itself.

With σ set to unity, the pseudo-moments remain the original moments, and the retrieved lognormals are of zero width. Use of these "tri-disperse" distributions is then equivalent to a 3-point quadrature evaluation of the optical integrals to be computed, and is the method

of McGraw *et al.* (1995). Thus if in the present approach lognormal model distributions are employed, the MIDAS technique may be viewed as a *moment-preserving* "broadening" of the quadrature abscissas into 3 modes of finite width.

For a trimodal modified gamma distribution the pseudo-moments are

$$\omega_k = N_1 (b_1^{-1/s})^k + N_2 (b_2^{-1/s})^k + N_3 (b_3^{-1/s})^k , \tag{12}$$

and by the same procedure we obtain the modified gamma parameters as

$$\begin{aligned} N_i &= w_i \\ b_i &= r_i^{-s} \\ n_i &= n \quad \text{retrieval parameter (integer)} \\ s_i &= s \text{ retrieval parameter} \end{aligned} \tag{13}$$

Since the retrieval parameters σ and s may be varied continuously, there exists an infinite set of possible retrieved (trimodal) lognormals, and a multiply-infinite set of possible retrieved (trimodal) modified gammas consistent with a specified set of moments.

Although the technique has been described for the case of 6 moments and trimodal retrieved distributions, it can be applied to $2N$ moments and N-modal retrieved distributions if higher moments are available (we have done so for up to $N = 6$), but as higher moments are not often available this has been investigated only briefly.

The technique now proceeds by retrieving distributions over a range of the model distribution retrieval parameters and then averaging those distributions. How the range of values for each retrieval parameter is to be chosen must be specified to fully define the method, and the following guidelines are empirical rules derived by trial and error (and are not necessarily the best possible):

Lognormals: Average (with equal weight) over all retrieved distributions with $1.1 \leqslant \sigma \leqslant \sigma_{\max}$, where $\sigma_{\max}$ is the largest value permitted by ORTHOG.

Modified gammas ($n = 6$): Average (with equal weight) over all retrieved distributions with $s_{\min} \leqslant s \leqslant s_{\min} + 0.7$, where $s_{\min}$ is the smallest value permitted by ORTHOG.

"Permitted by ORTHOG" means that the output $\{w_i, r_i\}$ of the routine do in fact satisfy equation (10), which is checked for each retrieval. The amount by which the retrieval parameter is incremented between retrievals is not important provided it is small enough so that some 10 or more distributions are obtained. For modified gammas, s was incremented by 0.05, resulting in 15 retrievals for each test distribution. For lognormals, it was convenient to increment the variable $X = \exp[(\ln \sigma)^2/2]$ (rather than σ) with a constant increment of $\mathrm{d}X = 0.0002$, small enough to insure that at least 15 retrievals were obtained for each test distribution. (For some of the broader distributions this sometimes led to many more retrievals than necessary, and for these $\mathrm{d}X$ could have been increased.)

The lognormal rule serves to discard those distributions that are nearly tridisperse and thus possessing unphysically narrow "modes", and this was observed to improve accuracy. The use of $s_{\min}$ in the modified gamma rule was suggested by a few observations in which broad (and thus long-tailed) lognormals were used as test distributions. Small values of s give longer tails to the modified gammas and this gave somewhat better results. This suggests that taking the smallest values of s permitted by ORTHOG may allow the procedure to use the moments as an indicator of possible long-tailed underlying distributions and select retrieved distributions accordingly. Values of the modified-gamma n parameter other than 6 have not been systematically investigated. All sets of retrieved distributions in this work (except those for Fig. 2b) were obtained according to these rules.

Model distribution parameters consistent with a given set of moments can of course also be determined using standard iterative numerical techniques to minimize the (squared) differences of the actual moments and those computed from the retrieved parameters. The technique of Yue *et al.* (1997) employs a minimization scheme of this sort. Using the

conjugate-gradient minimization routines of Press *et al.* (1992), an iterative approach of this type was coded but this was found to be much less efficient than the ORTHOG-derived retrievals.

2.2. *Definition of optical properties*

The Mie routine of Bohren and Huffman (1983) was used to obtain the scattering efficiency, Q_{sca}, the extinction efficiency, Q_{ext}, the 180° backscattering efficiency, Q_{B}, and the angular distribution of scattered light from a single particle for unpolarized incident light, $S_{11}(r, \theta)$, for each particle size required. From these the following properties were calculated for each test and average-retrieved distribution. (The wavelength and index of refraction dependence of all properties is suppressed.)

The extinction coefficient for a distribution, or the total cross section per unit volume, is

$$K_{\mathrm{ext}} = \pi \int r^2 \, Q_{\mathrm{ext}}(r) f(r) \, \mathrm{d}r, \tag{14}$$

and the 180° backscattering cross section is

$$\sigma_{\mathrm{B}} = \pi \int r^2 \, Q_{\mathrm{B}}(r) f(r) \, \mathrm{d}r. \tag{15}$$

The hemispheric backscatter fraction for isotropically incident radiation, β_{H}, is computed from equation (15b) of Wiscombe and Grams (1976):

$$\beta_{\mathrm{H}}(r) = \frac{1}{2\pi} \int_0^{\pi} \theta \, P(\theta) \sin\theta \, \mathrm{d}\theta \, , \tag{16}$$

where the scattering phase function is (Bohren and Huffman, 1983)

$$P(\theta) = N \int S_{11}(r, \theta) f(r) \, \mathrm{d}r \tag{17}$$

and N is a constant such that $P(\theta)$ is normalized over all scattering directions to 4π.

The asymmetry parameter, g_{asym}, and the upscatter fraction, β_{U}, were averaged over the distribution according to a scattering-efficiency-weighted average,

$$\phi = \frac{\pi \int r^2 Q_{\mathrm{sca}}(r) \, \phi(r) f(r) \, \mathrm{d}r}{\pi \int r^2 Q_{\mathrm{sca}}(r) f(r) \, \mathrm{d}r} = \frac{\pi \int r^2 Q_{\mathrm{sca}}(r) \, \phi(r) f(r) \, \mathrm{d}r}{K_{\mathrm{sca}}}, \tag{18}$$

as in McGraw *et al.* (1995), and expressions for $\phi(r)$ for these quantities can also be obtained from Wiscombe and Grams (1976). For the asymmetry parameter, $\phi \to g_{\mathrm{asym}}$ and $\phi(r) \to g(r)$ with

$$g(r) = \frac{1}{2} \int_0^{\pi} \cos\theta \, S_{11}(r, \theta) \sin\theta \, \mathrm{d}\theta \, , \tag{19}$$

and for the upscatter fraction (monodirectional incident radiation), $\phi \to \beta_{\mathrm{U}}$ and $\phi(r) \to \beta_{\mathrm{U}}(r, \theta_0)$ with

$$\beta_{\mathrm{U}}(r, \theta_0) = \frac{1}{2\pi} \int_{\pi/2 - \theta_0}^{\pi/2 + \theta_0} S_{11}(r, \theta) \sin\theta \cos^{-1}(\cot\theta_0 \cot\theta) \, \mathrm{d}\theta + \frac{1}{2} \int_{\pi/2 + \theta_0}^{\pi} S_{11}(r, \theta) \sin\theta \, \mathrm{d}\theta \tag{20}$$

where θ_0 is the solar zenith angle. $\beta_{\mathrm{U}}(r, \theta_0)$ is the fraction of radiation scattered in the upward direction, and it is this quantity rather than the fraction scattered into the backward hemisphere relative to the direction of incident radiation that is important in climate studies (Schwartz, 1995). A solar zenith angle of 30° was used throughout this study as this value is small enough to give the upscatter fraction a substantial dependence on particle size

(see Fig. 5 of Nemesure *et al.*, 1995); at $\theta_0 = 90^\circ$ (Sun at the horizon), $\beta_U(r,\theta_0)$ is independent of particle size by symmetry and would not be sensitive to the size distribution, as is desirable for the evaluation of retrieval techniques.

The sulfate scattering coefficient per unit sulfate mass (mass scattering efficiency) was evaluated as

$$\alpha_{SO_4^{-2}} = \frac{\pi \int r^2 Q_{sca}(r) f(r)\, dr}{\int m(r) f(r)\, dr} = \frac{K_{sca}}{(4\pi d/3)\, \mu_3} \tag{21}$$

where $m(r)$ is the sulfate mass in a particle of radius r and d is the sulfate concentration as described below. Sulfate mass per particle was calculated as in Boucher *et al.* (1998) and was based upon an assumed saturated ammonium sulfate solution at 80% relative humidity and 25°C, and obtained as sulfate concentration in solution times particle volume. The sulfate concentration for this solution is 540 g ammonium sulfate per liter (Tang and Munkelwitz, 1994), yielding $d = 0.3927$ g SO_4^{-2} cm^{-3}.

At a specified temperature, relative humidity, solar zenith angle, aerosol composition and wavelength, the direct (clear sky) shortwave forcing of a unit volume of aerosol (W cm^{-3}) is proportional to (Charlson *et al.*, 1992; Nemesure *et al.*, 1995) a quantity denoted as reduced forcing:

$$\Delta f_R = \pi \int r^2 Q_{sca}(r)\ \beta_U(r, \theta_0) f(r)\, dr\,. \tag{22}$$

In light of equation (18) the reduced forcing may be obtained as $\Delta f_R = K_{sca}\, \beta_U$. [The averaged quantity β_U should not be confused with the size-dependent quantity $\beta_U(r, \theta_0)$.] The appropriate value of the solar zenith angle would be the one that actually obtains at the particular time and location of the aerosol under consideration.

The computer code for calculating optical properties was checked by reproducing the values of K_{ext}, g_{asym}, β_H, and σ_B reported in McGraw *et al.* (1995), values of $\beta_U(r, \theta_0)$ reported in Nemesure *et al.* (1995), and values of $\alpha_{SO_4^{-2}}$ reported in Boucher *et al.* (1998).

3. RESULTS

3.1. *Test distributions*

Figure 1 shows the 28 test distributions derived from field observations collected for this study and the Appendix briefly describes the source and manner of treatment of each. These represent a variety of aerosol types and distribution shapes, and include urban, (clean) continental, and stratospheric aerosols, with most of them marine. Most were scanned and digitized from plots, smoothed, and converted from $dN/d\log D$ to dN/dr for use in the computer code. The results obtained for all distributions collected are presented here. The variability of the accuracy of the techniques over the set of distributions illustrates the usefulness of employing a large number of test distributions in assessing retrieval methods.

Figure 2a and c shows representative retrieved lognormal and modified gamma distributions and the average-retrieved distributions for test distribution 23, a marine distribution (Hoppel *et al.* 1990) employed previously in McGraw *et al.* (1995) and Yue *et al.* (1997). Thus panels 2a and c jointly show 19 distributions having the same first 6 moments. Note that neither the retrieved distributions nor their average are in especially close agreement with the test distribution, yet the surrogate distribution yields accurate estimates for all of the optical properties examined here.

3.2. *Single-wavelength evaluations*

Following McGraw *et al.* (1995) and Yue *et al.* (1997), this study was begun with $\lambda = 632.8$ nm and $n = 1.55 - 0\,i$ for single-wavelength computations. As there is no absorption (the imaginary part of the refractive index is zero), $K_{ext} = K_{sca}$ and $\alpha_{SO_4^{-2}}$ differs from

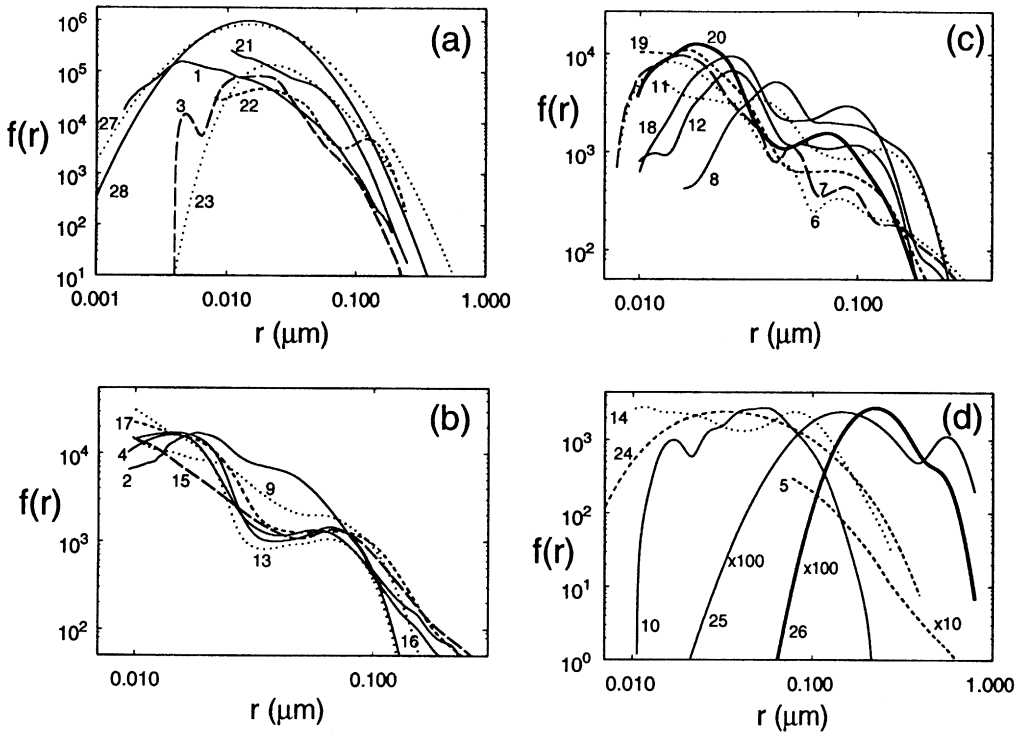

Fig. 1. The test distributions are grouped by maximum amplitude to facilitate compact presentation. Units are $\mu m^{-1}\,cm^{-3}$. All horizontal and vertical scales are logarithmic. The distributions with "$\times 10$" and "$\times 100$" in (d) have been scaled up for presentation purposes.

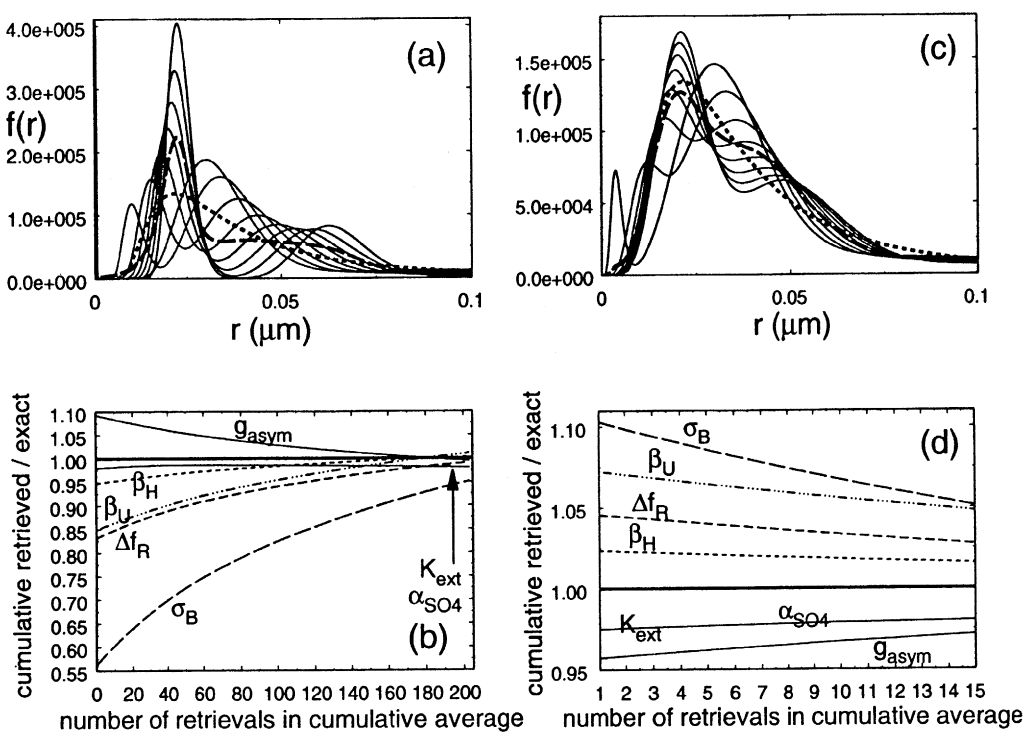

Fig. 2. (a) The dotted curve is test distribution 23. The solid curves are representative lognormal distributions retrieved from the moments of distribution 23. The dashed curve is the average of all retrieved lognormals for distribution 23, including those not shown. (b) Evolution of the ratio of the retrieved optical property to the exact result, for each optical property, as a function of the number of retrieved distributions. Intercepts on the vertical axis are the 3-point quadrature results. (c) Same as (a) but for retrieved modified gamma distributions. (d) Same as (b) but for retrieved modified gammas, and the quadrature results are not shown. Units for distributions are $\mu m^{-1}\,cm^{-3}$.

K_{ext} only by an overall normalization by the total sulfate mass in the aerosol and the errors in K_{ext} and $\alpha_{SO_4^{-2}}$ are the same.

Figure 2b is an illustrative figure showing the evolution of the ratios of the retrieved optical property to the exact result for distribution 23, for lognormal retrieved distributions. For this figure the 3-point quadrature results are the vertical intercepts, and the lognormal retrievals begin at $X = 1.0002$ ($\sigma = 1.0202$ rather than $\sigma = 1.1$) and are successively broadened in subsequent retrievals. This panel shows that the retrieved optical properties tend to converge toward the exact results as the average-retrieved distribution develops and the retrieved lognormals become broader. This convergence is characteristic whenever the quadrature errors are substantial. Thus beginning the lognormal retrievals at $\sigma = 1.1$ (rather than $\sigma = 1.0202$) eliminates those retrievals that give the poorest results.

Figure 2d is analogous to Fig. 2c for the case of retrieved modified gammas. Note that the modified gammas do not have the continuity with the quadrature results (which are not shown in this panel) as is the case with lognormals, since modified gammas do not have the 'delta-function' limit as do lognormals as $\sigma \to 1$. It is characteristic that the retrieved optical properties vary much less as the cumulative average develops for modified gammas than for lognormals.

Panels a and c of Figs 3–8 show how the computed optical properties of both the MIDAS and quadrature techniques track the exact results over the set of test distributions. The lower panels in each of these figures give the ratio of the retrieved optical property to the

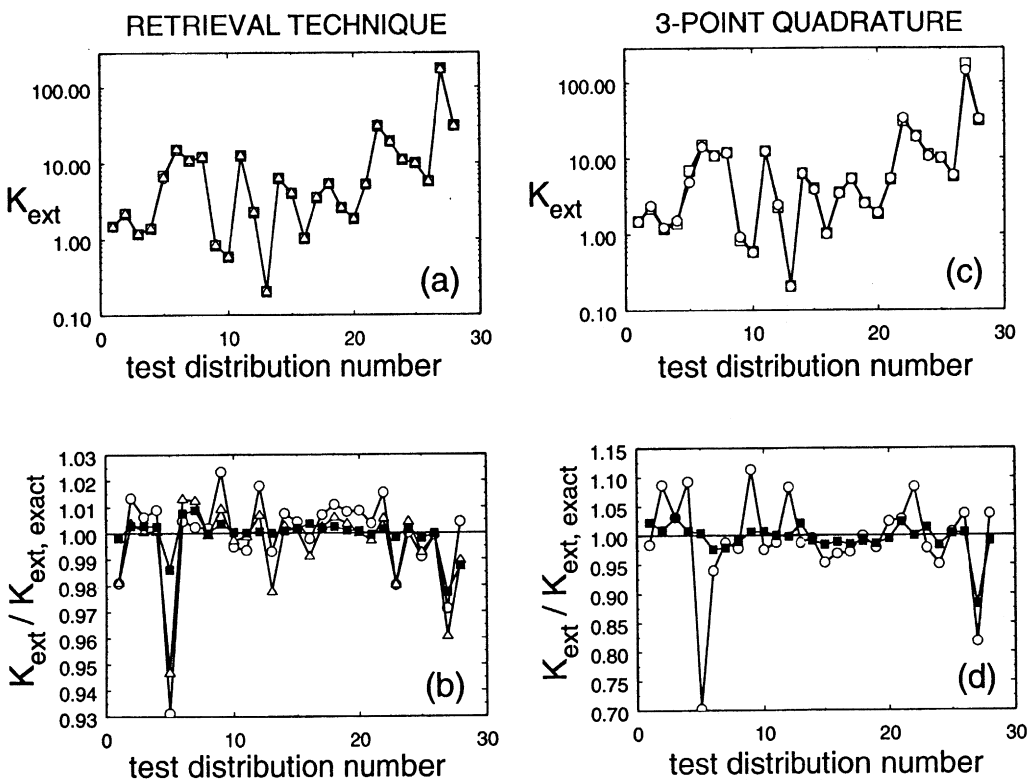

Fig. 3. Extinction coefficient, K_{ext}, ($\mu m^2\ cm^{-3}$) for each of the test distributions. (a) Squares are the exact results, circles the retrieved lognormal results, and triangles the retrieved modified gamma results, at $\lambda = 632.8$ nm and $n = 1.55 - 0\ i$. (b) Ratio of the retrieved result to the exact result for each distribution. Circles are for lognormals, triangles for modified gammas, and filled squares for the modified gammas averaged over the solar spectrum of Coakley *et al.* (1983). The values shown in this panel are also those obtained for the mass scattering efficiency, $\alpha_{SO_4^{-2}}$. (c) Squares are the exact results and circles the 3-point quadrature results at $\lambda = 632.8$ nm and $n = 1.55 - 0\ i$. (d) Ratio of the quadrature result to the exact result for each distribution. Circles are the single wavelength results and filled squares the results averaged over the solar spectrum. This panel also applies to ($\alpha_{SO_4^{-2}}$).

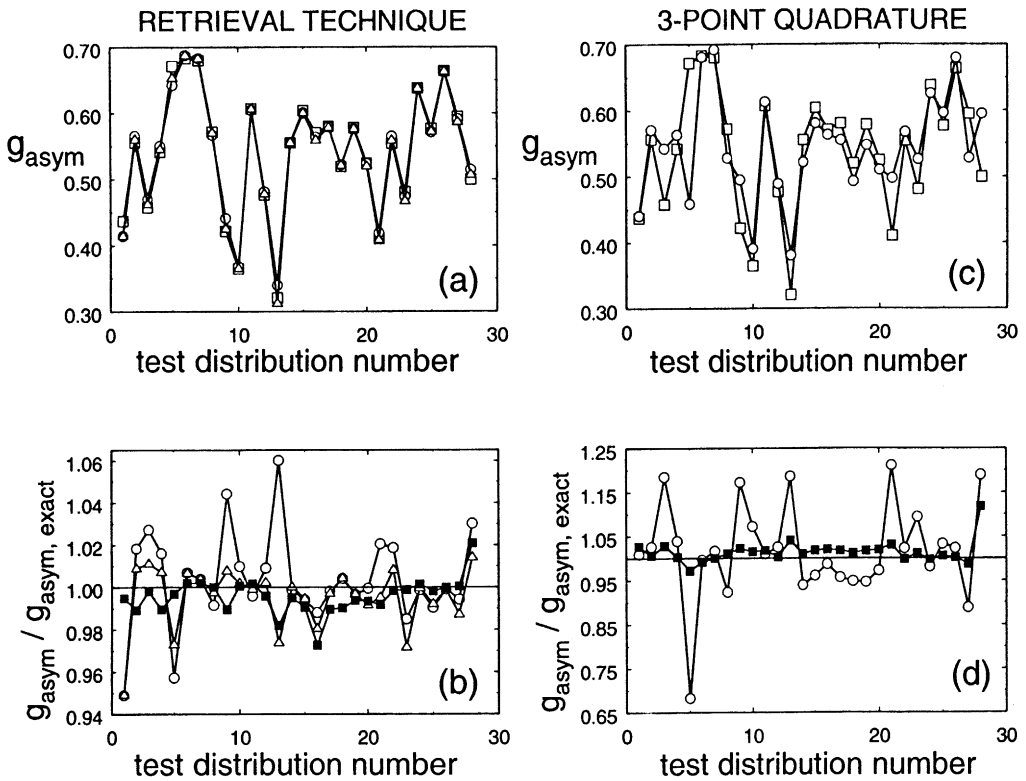

Fig. 4. Asymmetry parameter, g_{asym}, for each of the test distributions. Other details same as in Fig. 3.

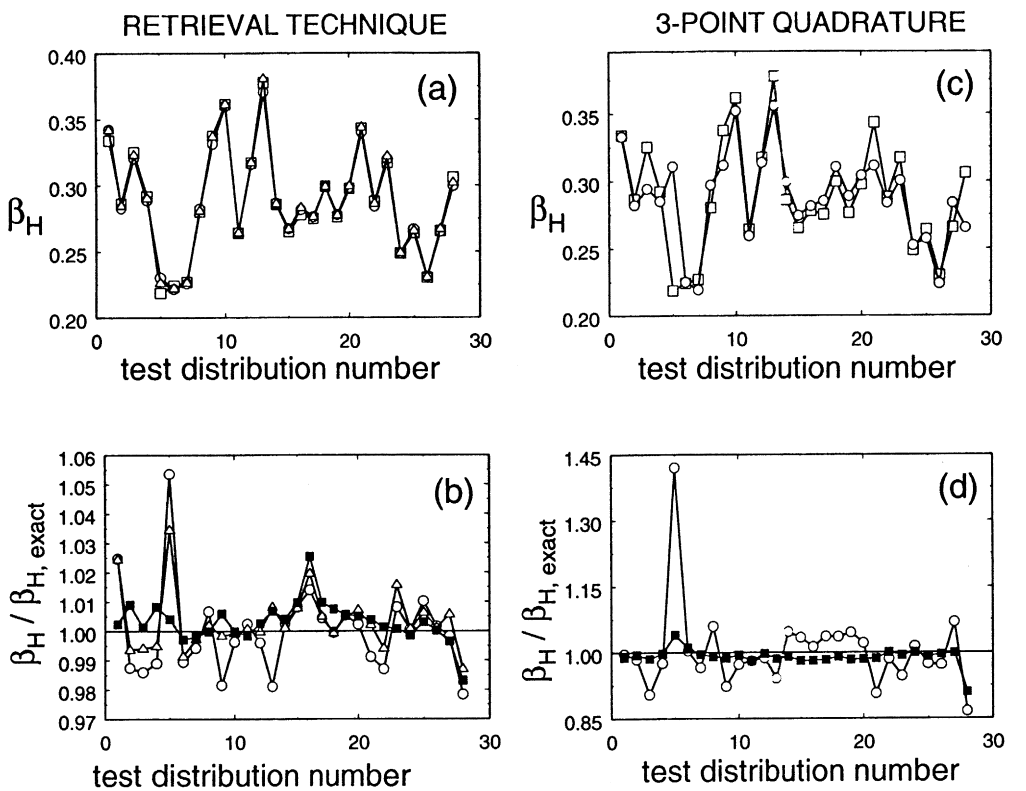

Fig. 5. Hemispheric backscatter fraction, β_{H}, for each of the test distributions. Other details same as in Fig. 3.

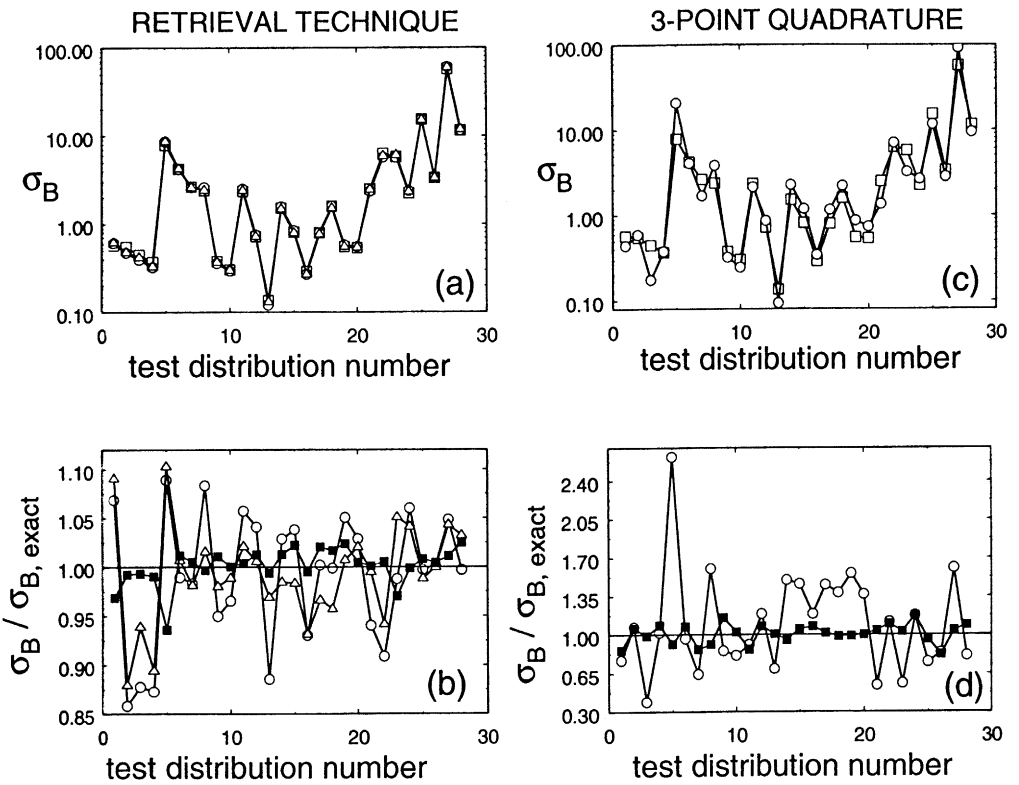

Fig. 6. 180° backscattering cross section, σ_B, ($\mu m^2\ cm^{-3}$) for each of the test distributions. Other details same as in Fig. 3.

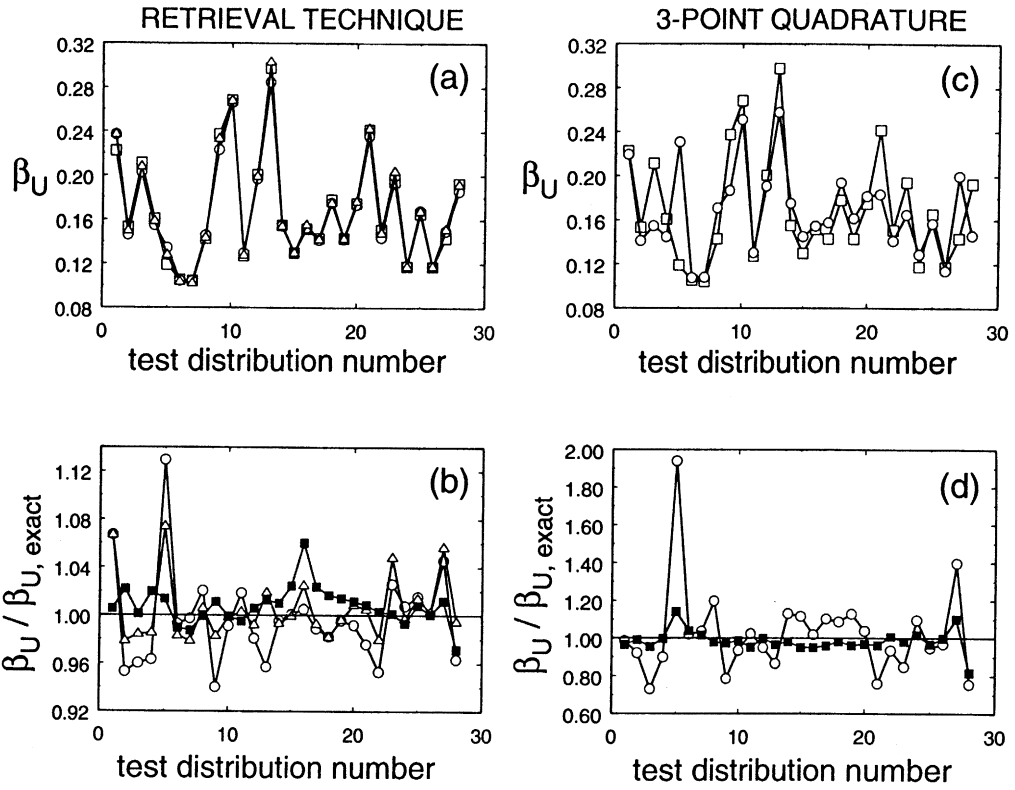

Fig. 7. Upscatter fraction, β_U, for each of the test distributions. Other details same as in Fig. 3.

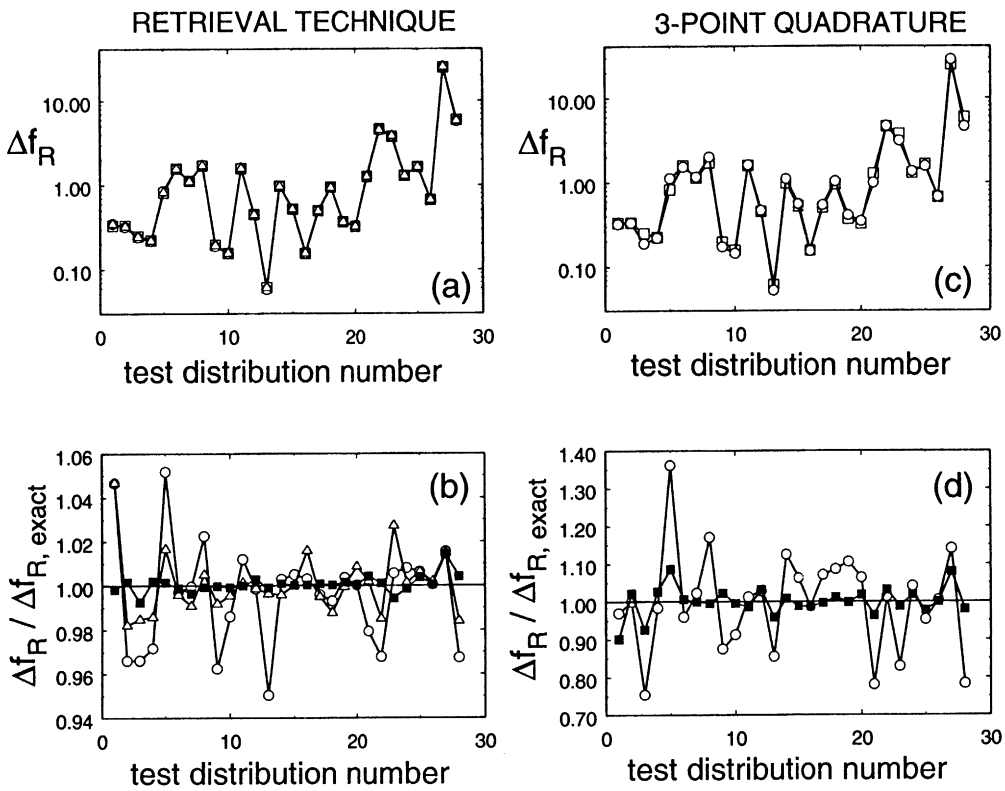

Fig. 8. Reduced forcing per unit volume, Δf_R, (μm^2 cm^{-3}) for each of the test distributions. Other details same as in Fig. 3.

exact result for each approach. Note the differing range of the ordinate for panels b and d in each of these figures.

Table 1 summarizes the performance of the MIDAS and quadrature methods by presenting the maximum error incurred, the average magnitude of the error (errors of opposite sign do not cancel), and the average error (errors of opposite sign cancel) for each property.

3.3. *Results averaged over the solar spectrum*

In many applications it is appropriate to average over the solar spectrum and this has been done with the retrieved modified gamma and quadrature techniques, in addition to the single wavelength evaluations reported above. Table 2 shows the Coakley *et al.* (1983) representation of the solar spectrum employed (with index of refraction $n = 1.40 - 0\ i$, independent of wavelength), and the optical properties averaged over this spectrum are shown in the lower panels of Figs 3–8 (solid boxes). Table 1 includes error statistics over the set of test distributions for these wavelength-averaged properties.

4. DISCUSSION AND CONCLUSIONS

4.1. *Single-wavelength evaluations*

Examination of Table 1 shows that at $\lambda = 632.8$ nm the maximum and average magnitude of error for the MIDAS technique are always smaller for the modified gammas than the lognormals. For the average error, where deviations of opposite sign cancel, there is little difference in accuracy for the two distribution types.

Table 1. Error statistics

	Maximum %error			Average magnitude of %error			Average %error		
	LN	MG	QD	LN	MG	QD	LN	MG	QD
Single wavelength evalution									
K_{ext}, $\alpha_{SO_4^{-2}}$,	−6.88	−5.32 (−5.32)	−29.76 (38.58)	1.13	0.93 (0.71)	5.22 (3.58)	−0.07	−0.42 (−0.12)	−0.78 (0.09)
g_{asym}	6.01	−5.08 (−8.91)	−31.77 (−31.78)	1.55	0.99 (1.12)	7.62 (5.40)	0.38	−0.44 (−0.54)	1.78 (1.06)
β_H	5.35	3.44 (5.59)	42.05 (42.05)	1.03	0.71 (0.71)	5.41 (3.82)	−0.001	0.34 (0.27)	0.31 (−0.67)
σ_B	−14.18	−12.04 (31.30)	161.72 (166.24)	5.20	3.78 (3.91)	34.88 (27.90)	−0.92	−0.63 (0.66)	10.11 (0.51)
β_U	12.95	7.39 (18.66)	93.91 (93.91)	2.70	1.82 (2.00)	14.43 (10.69)	−0.28	0.52 (0.46)	2.20 (0.05)
Δf_R	5.18	4.69 (16.04)	36.19 (36.19)	1.72	1.00 (1.51)	9.54 (9.27)	−0.41	0.07 (0.31)	−0.16 (−0.52)
Averages Over the Solar Spectrum									
K_{ext}, $\alpha_{SO_4^{-2}}$,		−2.25	−11.76		0.36	1.54		−0.04	−0.45
g_{asym}		−2.74	11.79		0.65	1.82		−0.44	1.44
β_H		2.54	−9.01		0.52	1.34		0.31	−0.97
σ_B		−6.39	−17.93		1.31	7.08		0.14	0.81
β_U		6.03	−18.30		1.26	3.82		0.80	−1.54
Δf_R		1.43	−9.83		0.23	2.56		0.06	0.04

Note. Column labels are '*LN*' for MIDAS (lognormals), '*MG*' for MIDAS (modified gammas), and '*QD*' for 3-point quadrature. For the single wavelength evaluations, the errors are the average or maximum values over the 28 test distributions at $\lambda = 632.8$ nm and $n = 1.55 - 0\,i$. In parentheses are the modified gamma and quadrature errors including all 8 wavelengths used in this study for each of the test distributions, based upon a total of $8 \times 28 = 224$ evaluations. For the results averaged over the solar spectrum the statistics are average or maximum values over the set of test distributions.

Table 2. Solar spectrum representation of Coakley *et al.* (1983) used in this study

λ, wavelength (nm)	f_λ, fraction of incident solar flux
340	0.0579
434	0.1389
508	0.0561
550	0.1527
768	0.1342
833	0.0881
991	0.0704

Table 3. Percent errors of the MIDAS (LN, MG), 3-point quadrature (QD) and Yue *et al.* (1997) (RSMT) techniques at $\lambda = 632.8$ nm and $n = 1.55 - 0\ i$ for the distributions employed in Yue *et al.* (1997)

	Dist. 23		Dist. 24		Dist. 25		Dist. 26	
	K_{ext}	σ_B	K_{ext}	σ_B	K_{ext}	σ_B	K_{ext}	σ_B
LN	−1.98	−1.22	0.02	6.03	−0.90	−0.28	−0.08	−0.18
MG	−1.98	−5.10	0.43	4.15	−0.73	−1.15	−0.05	−0.01
QD	−2.14	−44.2	−4.90	17.5	0.61	−24.8	3.71	−16.2
RSMT	−2.22	4.26	−2.20	−2.55	1.61	−0.92	0.19	−2.48

The values in parentheses in Table 1 are average or maximum values for the modified gamma retrieval or quadrature techniques employing all 8 wavelengths used in this study, and to the extent that calculations at different λ of this well-spaced set of wavelengths are independent, these statistics are over $8 \times 28 = 224$ independent evaluations. For these 224 evaluations, the errors in K_{ext} ($\alpha_{SO_4^{-2}}$), g_{asym} and β_H never exceed 5.3, 8.9 and 5.6%, respectively, for the modified gammas, and the average magnitude of error is less than 1% for each of these properties. Although the maximum errors for σ_B, β_U and Δf_R are somewhat larger, the average magnitude of error for these properties is about an order of magnitude smaller and indicates that errors as large as the maximum are not frequent. For both retrieved lognormals and modified gammas, the average error of each quantity is less than 1%.

Although the errors with 3-point quadrature can on occasion be somewhat large, the average magnitude of error remains under 10% for all properties except σ_B and β_U, and the average error does not exceed 1.1% for any calculated property when considering all 224 evaluations.

The Randomized Search Minimization Technique of Yue *et al.* (1997) also employs multiple retrievals of (histogram) distributions and obtains an average-retrieved distribution. Yue *et al.* (1997) evaluated K_{ext} and σ_B for distributions 23, 24, 25 and 26, (also at $\lambda = 632.8$ nm and $n = 1.55 - 0\ i$) and Table 3 cites those results along with the results of the MIDAS and quadrature methods. For these distributions the MIDAS results are somewhat more accurate for K_{ext}, with the Yue *et al.* (1997) and MIDAS results comparable for σ_B. The unusually small errors for the modified gammas for distribution 26 result from the fact that the average-retrieved distribution nearly coincides with the bimodal lognormal test distribution. For applications where single wavelength measurements are important, such as LIDAR, either the MIDAS or RSMT techniques would be recommended.

4.2. *Averages over the solar spectrum*

For retrieved modified gammas, averages over the solar spectrum of $K_{ext}(\alpha_{SO_4^{-2}})$, g_{asym}, β_H and Δf_R were always found to give errors less than 3%. The average magnitude of error did not exceed 1.3% for any of the wavelength-averaged properties, and the average error

did not exceed 0.8%. For the quadrature technique the average magnitude of error for all properties is less than 4%, excepting σ_B, and the average error never exceeded 1.5% in any calculated property.

In particular, for the MIDAS (quadrature) technique, the error in Δf_R did not exceed 1.43% (9.83%) for any test distribution, and to the extent that the 28 test distributions may be thought of as 28 neighboring grid cells in a large-scale 3-D model, the error in the aerosol part of the direct shortwave forcing integrated over that domain would be only 0.06% (0.04%), the average error in Δf_R. These grand averages over many distributions help establish the absence of systematic error in these techniques. Additionally, these averages show that for properties that are summed over significant portions of the model domain (such as radiative forcing) there should be substantial cancellation of errors.

To put these errors in perspective, Penner et al. (1994) estimate the uncertainties in $\alpha_{SO_4^{-2}}$ and β_U for sulfate aerosols as 40 and 30%, respectively, which combine (as independent errors) to give about 50% uncertainty in Δf_R from these quantities alone. These uncertainties result solely from lack of knowledge of the aerosol size distribution. The overall uncertainty for the clear sky forcing of anthropogenic sulfate aerosols was estimated to be greater than a factor of 2. Even with known (assumed) size distributions, the model intercomparisons of Boucher *et al.* (1998) show that computations with various radiative transfer models agree only to within about 8% at best. The present results show that knowledge of only the first 6 moments, rather than the full size distribution, results in minimal increase in uncertainties for the forcing and other optical properties relative to the uncertainties in present knowledge of the ambient aerosol properties and uncertainties in computing the radiative effects of known aerosol distributions.

4.3. *Computational efficiency*

For a hemispheric-scale Eulerian model with 1° resolution in the horizontal and 30 or so vertical levels there are roughly $360 \times 90 \times 30 = 972{,}000$ grid cells, each yielding a set of moments parameterizing the aerosol at each point in time at which the simulation data is to be analyzed. As it may be desirable to compute aerosol optical properties for each grid cell at many simulation times, computational efficiency will be important.

The quadrature technique has the advantage of requiring optical property computations for only three particle sizes (per set of moments). If average or integral properties over a substantial spatial domain are all that is required, even at a single wavelength, examination of the average errors in Table 1 shows that with the exception of σ_B, which is very sensitive to the particle size distribution, 3-point quadrature is nearly as accurate as the MIDAS technique, with all properties having average errors no greater than 2.2%. If incremental optical properties for the range of possible particle sizes are to be precomputed, a fine grid may be necessary in that the possible abscissas cannot be specified in advance for this form of Gaussian quadrature (with unknown weight functions).

For the MIDAS technique, obtaining the set of model distributions is rapid: 2000 + distributions per second have been retrieved on a Sun Spark Ultra-Enterprise or desktop PC with a 400 MHz Pentium II Processor. Evaluation of the optical properties of the retrieved model distributions will likely limit the overall efficiency, which is largely determined by the number of evaluation points (particle sizes) employed in the discretization of the distributions (50 per decade were used in these accuracy evaluations) and the amount of pre-computation. For computationally intensive applications a lookup table can be constructed with incremental optical properties for each evaluation point, and for each average-retrieved distribution one need only sum over the incremental properties with the appropriate weighting. Assuming the Randomized Search Minimization Technique and MIDAS techniques to be on equal footing regarding computing optical properties from their respective average-retrieved distributions (both may pre-compute incremental quantities), it is expected that the efficient ORTHOG routine gives the present technique significantly greater efficiency.

5. CONCLUSIONS

The effectiveness of the present technique is presumed to be due, at least in part, to the use of smooth distributions that go to zero at the smallest and largest particle sizes. Although some of the test distributions do not go to zero as the particle size is reduced due to instrumental detection limits, optical properties become progressively weaker with decreasing particle size and apparently these distribution shapes do not pose a problem for this approach. An exception is test distribution 5, which cuts off sharply at 0.074 μm, a particle size large enough to have appreciable scattering properties, and this distribution gives some of the largest errors for both the quadrature and retrieval techniques.

White (1990) and McGraw *et al.* (1998) have discussed sets of distributions having identical moments and a possible breakdown in the correlation of moments and aerosol dynamic and optical properties. Both of those studies involved families of distributions having a full (infinite) set of identical moments. As pointed out by McGraw *et al.* (1998), for very broad multimodal distributions the moment-optical property correlation needs further investigation, and it may prove necessary to represent each aerosol mode with a separate set of moments to maintain the correlation. A recent calculation of Vasconcelos *et al.* (1998) suggests that this indeed may be the case.

In the present study the retrieved distributions have only 6 moments in common, and there is thus a greater range of variation among the possible retrieved distrib utions. Although the full space of retrieved distributions for a set of moments has not been explored, the extent to which optical properties vary among the retrieved distributions in a set can be judged to some extent from Fig. 2, bearing in mind that these are cumulative averages over a developing set of retrieved distributions. With the exception of σ_B, the optical properties of all retrieved distributions for test distribution 23 are within about 20% of the exact values. Although broader multimodal distributions have not been constructed and examined in this work, for the set of field distributions employed in this study the correlation between the lower moments and optical properties is strong.

As noted above, the lognormal version of the retrieval technique can be viewed as a moment-preserving broadening of the quadrature abscissas. As indicated in McGraw *et al.* (1995), the non-polynomial nature of the Mie kernels and their resonances can give sampling difficulties to the quadrature technique, having a few (discrete) abscissas. In fact, it is common practice when computing optical properties of monodisperse distributions to replace the monodisperse with a narrow lognormal to broaden over resonances. Simply taking the monodisperse radius as the geometric mean radius of a lognormal distribution, however, is not a moment-preserving operation, so that in retrieving aerosol optical properties from moments one may not simply do this for each of the quadrature abscissas. Moment-preserving broadening must be a concerted process involving all of the abscissas and will in general change both the abscissas and their respective weights. The broadening of the quadrature abscissas with retrieved lognormals apparently overcomes the sampling problem while preserving the moments. More generally, the lognormal version of the MIDAS technique might be viewed as an extension of quadrature techniques for non-smooth integrands and other applications are under investigation.

An efficient technique for obtaining smooth model distributions consistent with an arbitrary (even) number of moments should have application in aerosol dynamics modeling. As a closure technique for the coupled equations of the method of moments (McGraw and Saunders, 1984; Pratsinis, 1988; Barrett and Jheeta, 1996; McGraw, 1997; Barrett and Webb, 1998) the use of retrieved distributions derived from 4 or more moments would be an extension of the single-lognormal 3-parameter closure often used and characteristic of the Modal Aerosol Dynamics approach to aerosol modeling (Whitby and McMurry (1997) and references therein). Yue *et al.* (1997) notes that the first 4 moments are clearly inferior to the first 6 for retrieving aerosol optical properties, and even though the condensation and coagulation kernels encountered in aerosol dynamics are smoother than the Mie kernels, higher moments may be useful in modeling dynamics as well. The MIDAS technique may also provide a means for the method of moments to model CCN activation and the cloud

processing of atmospheric aerosols. A set of retrieved distributions, each of which consistent with the modeled moments, would in a sense be appropriate to represent the aerosol in a single grid cell, considering the wide sub-grid variability in aerosol properties. It is worth noting that lognormals and modified gammas are probably not the only model distribution types that can be retrieved with this technique. Applications to aerosol dynamics will be the topic of a forthcoming report.

It is concluded that with the possible exception of very broad distributions, the lower moments contain sufficient information about the particle size distribution to constrain the optical properties to within fairly narrow bounds. The MIDAS technique presented in this paper, as well as the quadrature and Randomized Search Minimization Technique techniques previously described, provides an accurate means of obtaining aerosol optical properties from the lower moments of the size distribution. Although the MIDAS and RSMT techniques are recommended for single wavelength computations where spatial and/or spectral averaging is undesirable, the quadrature technique appears to be of nearly equal accuracy when averaging or integrating over a spatial domain containing many distinct aerosol samples.

Acknowledgements—The author would like to thank Robert McGraw for many fruitful discussions and for making his McGraw *et al.* (1995) notes available, Stephen Schwartz for discussions and comments on this manuscript, and Rodney Weber for providing field observation data. The author is glad to acknowledge the essential contribution of the authors of *Numerical Recipes* to this work. This research was supported in part by NASA through interagency agreement number W-18,429 as part of its interdisciplinary research program on tropospheric aerosols, and in part by the Environmental Sciences Division of the US Department of Energy (DOE) as part of the Atmospheric Radiation Measurement Program, and was performed under the auspices of DOE Contract No. DE-AC0298CH10886.

REFERENCES

Barrett, J. C. and Jheeta, J. S. (1996) Improving the accuracy of the moments method for solving the aerosol general dynamic equation. *J. Aerosol Sci.* **27,** 1135–1142.

Barrett, J. C. and Webb, N. A. (1998) A comparison of some approximate methods for solving the aerosol general dynamic equation. *J. Aerosol Sci.* **29,** 31–39.

Bates, T. S., Kapustin, V. N., Quinn, P. K., Covert, D. S., Coffman, D. J., Mari, C., Durkee, P. A., De Bruyn, W. J. and Saltzman, E. S. (1998) Processes controlling the distribution of aerosol particles in the lower marine boundary layer during the First Aerosol Characterization Experiment (ACE 1). *J. Geophys. Res.* **103,** 16,369–16,383.

Benkovitz, C. M., Berkowitz, C. M., Easter, R. C., Nemesure, S., Wagener, R. and Schwartz, S. E. (1994) Sulfate over the Atlantic and adjacient continental regions: evaluation of October and November 1986 using a three-dimensional model driven by observation-derived meteorology. *J. Geophys. Res.* **99,** 20,725–20,756.

Bohren, C. F. and Huffman, D. R. (1983) *Adsorption and Scattering of Light by Small Particles.* Wiley, New York.

Boucher, O., Schwartz, S. E., Ackerman, T. P., Anderson, T. L., Bergstrom, B., Bonnel, B., Chylek, P., Dahlback, A., Fouquart, Y., Fu, Q., Halthore, R. N., Haywood, J. M., Iversen, T., Kato, S., Kinne, S., Kirkavag, A., Knapp, K. R., Lacis, A., Laszlo, I., Mishchenko, M. I., Nemesure, S., Ramaswamy, V., Roberts, D. L., Russell, P., Schlesinger, M. E., Stephens, G. L., Wagener, R., Wang, M., Wong, J. and Yang, F. (1998) Intercomparison of models representing direct shortwave radiative forcing by sulfate aerosols. *J. Geophys. Res.* **103,** 16,979–16,998.

Brechtel, F. J., Kreidenweis, S. M. and Swan, H. B. (1998) Air mass characteristics, aerosol particle number concentrations, and number size distributions at Macquarie Island during the First Aerosol Characterization Experiment (ACE 1). *J. Geophys. Res.* **103,** 16,351–16,367.

Charlson, R. J., Schwartz, S. E., Hales, J. M., Cess, R. D., Coakley, J. A., Hansen, J. E. and Hofmann, D. J. (1992) Climate forcing by anthropogenic aerosols. *Science* **255,** 423–430.

Clarke, A. D., Li, Z. and Litchy, M. (1996) Aerosol dynamics in the equatorial Pacific Marine boundary layer: Microphysics, diurnal cycles and entrainment. *Geophys. Res. Lett.* **23,** 733–736.

Coakley, J. A., Cess, R. D. and Yurevich, F. B. (1983) The effect of tropospheric aerosols on the earth's radiation budget: A parameterization for climate models. *J. Atmos. Sci.* **40,** 116–138.

Covert, D. S., Gras, J. L., Wiedensohler, A. and Stratmann, F. (1998) Comparison of directly measured CCN with CCN modeled from the number-size distribution in the marine boundary layer during ACE 1 at Cape Grim, Tasmania. *J. Geophys. Res.* **103,** 16,597– 16,608.

Deshler, T. B., Johnson, B. J. and Rozier, W. R. (1993) Balloonborne measurements of Pinatubo aerosol during 1991 and 1992 at 41°N; vertical profiles, size distribution, and volatility. *Geophys. Res. Lett.* **20,** 1435–1438.

Deuze, J. L., Herman, M., Goloub, P., Tanre, D. and Marchand, A. (1998) Characterization of the aerosol over the ocean from POLDER, *Geophys. Res. Lett.* (submitted).

Feller, W. (1971) *An Introduction to Probability Theory and Its Applications*, Vol. II, p. 155, Wiley, New York.

Goloub, M., Tanre, P., Deuze, J. L., Herman, M. and Marchand, A. (1998) Validation of the first algorithm applied for deriving the aerosol properties over the ocean using the POLDER/ADEOS measurements. *IEEE Trans. Geosci. Remote Sens.* (accepted).

Hegg, D. A., Ferek, R. J. and Hobbs, P. V. (1993) Aerosol size distributions in the cloudy atmospheric boundary layer of the North Atlantic Ocean. *J. Geophys. Res.* **98,** 8841–8846.
Heintzenberg, J., Muller, H., Quenzel, H. and Thomalla, E. (1981) Information content of optical data with respect to aerosol properties: numerical studies with a randomized minimization-search-technique inversion algorithm. *Appl. Opt.* **20,** 1308–1315.
Hoppel, W. A., Fitzgerald, J. W., Frick, G. M. and Larson, R. E. (1990) Aerosol size distributions and optical properties found in the marine boundary layer over the Atlantic ocean. *J. Geophys. Res.* **95,** 3659–3686.
Kaufman, Y. J., Tanre, D., Remer, L., Vermote, E., Chu, A. and Holben, B. N. (1997) Remote sensing of tropospheric aerosol from EOS-MODIS over the land using dark targets and dynamics aerosol models. *J. Geophys. Res.* **102,** 17051–17067.
Livingston, J. M. and Russel, P. B. (1989) Retrieval of aerosol size distribution moments from multiwavelength particulate extinction measurements. *J. Geophys. Res.* **94,** 8425–8433.
McGraw, R. and Saunders, J. H. (1984) A condensation feedback mechanism for oscillatory nucleation and growth, *Aerosol Sci. Technol.* 367–380.
McGraw, R. (1997) Description of aerosol dynamics by the quadrature method of moments, *Aerosol Sci. Technol.* **27,** 255–265.
McGraw, R., Huang, P. I. and Schwartz, S. E. (1995) Optical properties of atmospheric aerosols from moments of the particle size distribution. *Geophys. Res. Lett.* **22,** 2929–2932.
McGraw, R., Nemesure, S. and Schwartz, S. E. (1998) Properties and evolution of aerosols with size distributions having identical moments. *J. Aerosol Sci.* **29,** 1–12.
Nemesure, S., Wagener, R. and Schwartz, S. E. (1995) Direct shortwave forcing of climate by the anthropogenic sulfate aerosol: Sensitivity to particle size, composition, and relative humidity. *J. Geophys. Res.* **100,** 26,105–26,116.
Overbeck, V. R., Danielson, E. F., Snetsinger, K. G., Ferry, G. V., Fong, W. and Hayes, D. M. (1983) Effect of the eruption of El Chichon on stratospheric aerosol size and composition. *Geophys. Res. Lett.* **10,** 1021–1024.
Parungo, F. P., Nagamoto, C. T., Rosinski, J. and Haagenson, P. L. (1986) A study of marine aerosols over the Pacific Ocean. *J. Atmos. Chem.* **4,** 199–226.
Penner, J. E., Charlson, R. J., Hales, J. M., Laulainen, N. S., Leifer, R., Novakov, T., Ogren, J., Radke, L. F., Schwartz, S. E. and Travis, L. (1994) Quantifying and minimizing uncertainty of climate forcing by anthropogenic aerosols. *Bull. Amer. Meteorolog. Soc.* **75,** 375–400.
Porter, J. N. and Clarke, A. D. (1997) Aerosol size distribution models based on in situ measurements. *J. Geophys. Res.* **102,** 6035–6045.
Press, W. H., Teukolsky, S. A., Vetterling, W. T. and Flannery, B. P. (1992) *Numerical Recipes in FORTRAN*. Cambridge University Press, Cambridge.
Pratsinis, S. E. (1988) Simultaneous nucleation, condensation, and coagulation in aerosol reactors. *J. Coll. Interface Sci.* **124,** 416–427.
Quinn, P. K., Kapustin, V. N., Bates, T. S. and Covert, D. S. (1996) Chemical and optical properties of marine boundary layer aerosol particles of the mid-Pacific in relation to sources and meteorological transport. *J. Geophys. Res.* **101,** 6931–6951.
Russell, L. M., Huebert, B. J., Flagan, R. C. and Seinfeld, J. H. (1996) Characterization of submicron size distributions from time-resolved measurements in the Atlantic Stratocumulus Transition Experiment/Marine Aerosol and Gas Exchange. *J. Geophys. Res.* **101,** 4469–4478.
Schwartz, S. E. (1995) The whitehouse effect—shortwave radiative forcing of climate by anthropogenic aerosols: an overview. *J. Aerosol Sci.* **27,** 359–382.
Tang, I. N. and Munkelwitz, H. R. (1994) Water activities, densities, and refractive indicies of aqueous sulfates and sodium nitrate droplets of atmospheric importance. *J. Geophys. Res.* **99,** 18,801–18,808.
Vasconcelos, L. A. de P., Macias, E. S. and White, W. H. (1998) On the relationship of aerosol optics to moments of particle size distribution. *Geophys. Res. Lett.* **25,** 4189–4192.
Weber, R. J. and McMurry, P. H. (1996) Fine particle size distributions at the Mauna Loa observatory, Hawaii. *J. Geophys. Res.* **101,** 14,767–14,775.
Weber, R. J., Marti, J. J., McMurry, P. H., Eisele, F. L., Tanner, D. J. and Jefferson, A. (1997) Measurements of new particle formation and ultrafine particle growth rates at a clean continental site. *J. Geophys. Res.* **102,** 4375–4385.
Weber, R. J., McMurry, P. H., Mauldin, L., Tanner, D. J., Eisele, F. L., Brechtel, F. J., Kreidenweis, S. M., Kok, G. L., Schillawski, R. D. and Baumgardner, D. (1998) A study of new particle formation and growth involving biogenic and trace gas species measured during ACE 1. *J. Geophys. Res.* **103,** 16,385–16,396.
Whitby, E. R. and McMurry, P. H. (1997) Modal aerosol dynamics modeling. *Aerosol Sci. Technol.* **27,** 673–688.
Whitby, K. T. (1978) The physical characteristics of sulfur aerosols. *Atmos. Environ.* **12,** 125–159.
White, W. H. (1990) Particle size distributions that cannot be distinguished by their integral moments. *J. Coll. Interface Sci.* **135,** 297–299.
Wiscombe, W. and Grams, G. (1976) The backscattered fraction in two-stream approximations. *J. Atmos. Sci.* **33,** 2440–2451.
Yue, G. K., Lu, J., Mohnen, V. A., Wang, P.-H., Saxena, V. K. and Anderson, J. (1997) Retrieving aerosol optical properties from moments of the particle size distribution. *Geophys. Res. Lett.* **24,** 651–654.

APPENDIX A: THE TEST DISTRIBUTIONS

The description of each distribution includes the set of values (r_L, r_U, R_L, R_U), all in micrometers. r_L and r_U are the lower and upper limits of integration used to compute the moments of the test distribution, which were determined by the field data, limitations in scanning the distributions from the figures, and values used in McGraw *et al.* (1995) and Yue *et al.* (1997). R_L and R_U are the lower and upper limits of integration used when integrating optical properties over the average-retrieved distributions and were chosen large enough for convergence.

Distribution 1. Covert *et al.* (1998), marine distribution from Fig. 2, curve d, (0.00163, 0.195, 0.0001, 1.9).
Distribution 2. Weber *et al.* (1998), marine distribution from Fig. 2, dashed curve, (0.00941, 0.251, 0.0001, 2.5).
Distribution 3. Bates *et al.* (1998), of continental origin, from Fig. 3a, (0.00396, 0.254, 0.0001, 2.5).
Distribution 4. Brechtel *et al.* (1998), marine (Macquarie Island) distribution from Fig. 4, solid curve, (0.00934, 0.246, 0.0001, 2.5).
Distribution 5. Parungo *et al.* (1986), marine distribution from Fig. 7, 3rd panel, solid curve, (0.0738, 3.74, 0.0001, 10.0).
Distribution 6. Russell *et al.* (1996), marine distribution from Fig. 6, bottom curve, (0.00798, 0.500, 0.0001, 5.0).
Distribution 7. Russell *et al.* (1996), marine distribution from Fig. 6, top curve, (0.00792, 0.450, 0.0001, 4.5).
Distribution 8. Clarke *et al.* (1996), marine distribution from Fig. 1, open boxes, (0.0157, 0.348, 0.0001, 3.5). This dry size distribution was converted to a "wet" distribution by scaling all particle sizes by a factor of 1.6.
Distribution 9. Hegg *et al.* (1993), marine distribution from Fig. 12, open circles, (0.00976, 0.282, 0.0001, 2.8).
Distribution 10. Hegg *et al.* (1993), marine distribution from Fig. 4, open circles, (0.0106, 0.223, 0.0001, 2.2).
Distribution 11. Porter *et al.* (1997), marine distribution from Fig. 4A, solid triangles, (0.0131, 0.364, 0.0001, 3.6).
This dry size distribution was converted to a "wet" distribution by scaling all particle sizes by a factor of 1.6.
Distributions 12-20. Quinn *et al.* (1996), marine distributions.
Distribution 12, Fig. 4d, (0.00998, 0.278, 0.0001, 2.8)
Distribution 13, Fig. 4b, (0.00986, 0.218, 0.0001, 2.2)
Distribution 14, Fig. 4e, (0.00984, 0.281, 0.0001, 2.8)
Distribution 15, Fig. 4f, (0.0100, 0.285, 0.0001, 2.8)
Distribution 16, Fig. 4c, (0.00991, 0.277, 0.0001, 2.8)
Distribution 17, Fig. 5a, (0.00991, 0.282, 0.0001, 2.8)
Distribution 18, Fig. 5d, (0.0100, 0.282, 0.0001, 2.8)
Distribution 19, Fig. 5b, (0.00999, 0.282, 0.0001, 2.8)
Distribution 20, Fig. 5c, (0.00979, 0.289, 0.0001, 2.9)
Distribution 21. Weber *et al.* (1997), clean continental distribution from Fig. 4a, curve "600-1000", (0.0107, 0.257, 0.0001, 2.6).
Distribution 22. Weber *et al.* (1996), marine distribution from Table 1, columns 3 and 5 (Fig. 5, lower panel), (0.00800, 0.250, 0.0001, 2.5).
Distribution 23. Hoppel *et al.* (1990), marine "distribution 1", fit to the form $\ln[f(r)] = C_0 + C_1(\ln r) + C_2(\ln r)^2 + \cdots$ with $C_0 = -2.1134$, $C_1 = -12.9179$, $C_2 = -11.9178$, $C_3 = -6.61389$, $C_4 = -1.52973$, (0.002, 0.200, 0.0001, 1.0).
Distribution 24. Hoppel *et al.* (1990), marine "distribution 4", fit to the form $\ln[f(r)] = C_0 + C_1(\ln r) + C_2(\ln r)^2 + \cdots$ with $C_0 = -3.08677$, $C_1 = -14.3583$, $C_2 = -13.2560$, $C_3 = -6.20314$, $C_4 = -1.21969$, (0.004, 0.400, 0.0001, 2.0).
Distribution 25. Overbeck *et al.* (1983), stratospheric distribution after the eruption of El Chichon in 1982; parameterization as a bimodal lognormal from Yue *et al.* (1997) with $N_1 = 5.10\ \mathrm{cm}^{-3}$, $N_2 = 2.80\ \mathrm{cm}^{-3}$, $R_1 = 0.19\ \mu$m, $R_2 = 0.59\ \mu$m, $\sigma_1 = 1.65$, and $\sigma_2 = 1.20$, (0.100, 0.800, 0.0001, 10.0)
Distribution 26. Deshler *et al.* (1983), stratospheric distribution after the eruption of Pinatubo in 1991; parameterization as a bimodal lognormal from Yue *et al.* (1997) with $N_1 = 5.25\ \mathrm{cm}^{-3}$, $N_2 = 0.56\ \mathrm{cm}^{-3}$, $R_1 = 0.25\ \mu$m, $R_2 = 0.53\ \mu$m, $\sigma_1 = 1.38$, and $\sigma_2 = 1.17$, (0.100, 0.800, 0.0001, 10.0)
Distribution 27. Whitby (1978), Table 1, distribution 6, "urban average" accumulation mode parametrized as a single lognormal with $N = 32{,}000\ \mathrm{cm}^{-3}$, $R = 0.027\ \mu$m and $\sigma = 2.16$, (0.0001, 0.800, 0.0001, 10.0). This dry sulfur aerosol distribution was not converted to a wet distribution as the index of refraction of dry ammonium sulfate is $n = 1.56$, and $n = 1.55$ was used in most of this study. (Note that the computation of the sulfate mass scattering efficiency treats all distributions as ammonium sulfate solutions, with the result that this property is underestimated for this distribution.)
Distribution 28. Whitby (1978), Table 1, distribution 8, "Labadie plume" accumulation mode parametrized as a single lognormal with $N = 30{,}000\ \mathrm{cm}^{-3}$, $R = 0.023\ \mu$m and $\sigma = 1.96$, (0.0001, 0.800, 0.0001, 10.0). The comments regarding distribution 27 apply here as well.